FDTD Analysis of an MIS Nanostructure Based Room-Temperature Plasmonic Laser

Md. Mesbahur Rahman and Md Zahurul Islam*
Department of Electrical & Electronic Engineering, BUET
Dhaka, Bangladesh
* mdzahurulislam@eee.buet.ac.bd

***Abstract*— Operation of plasmonic laser at room temperature has always been an issue towards its practical implementation and integration with electronic IC chip. In this work, we studied a room-temperature plasmonic laser configuration and semi classically evaluated their performances which are validated by previously reported experimental results. The laser structure employs an Metal-Insulator-Semiconductor hybrid nanostructure and effective cavity feedback mechanism to overcome the high metallic loss at room temperature by improving cavity Q factor. Optical pumping method is used the results show lasing action at room temperature from visible to ultraviolet range. Finite-Difference Time-Domain simulation method is used to solve the full-field vector Maxwell's equations on the laser structure and Four Level-Two Electron system is used to model the gain medium. All necessary data for the simulation are taken at room temperature to simulate the room temperature environment accurately. The results were found up to the mark of experimental data.**

Keywords*—*Room-temperature laser, plasmonic laser, MIS hybrid structure

I. INTRODUCTION

Despite all the recent efforts, size of lasers are still limited by the diffraction limit to be scaled accordingly to be integrated with their electronic IC counterpart [1]. In this respect, plasmonic lasers which obtain optical confinement and feedback using surface plasmon polaritons (SPPs), quasiparticles of electron and photon at metal dielectric interface, shows possibility in achieving sub-diffraction scale device [1-4]. However, fast electron collision & scattering in metal and low cavity feedback makes room-temperature operation of such device critical [1,2].

As usual, three things are necessary to make a laser - active gain medium, pumping requirements and optical feedback mechanism. Plasmonics can fundamentally contribute to the light confinement and optical feedback mechanism [5,6] at the metal-dielectric interface to reduce its size and light can be amplified by suitable gain medium. Several structures, such as MIM [7], distributed feedback cavity [8], whispering gallery cavity [9] can ensure feedback through one-dimensional confinement, while other structures, such as, hybrid Metal-Insulator-Semiconductor (MIS) nanowire structure [2] and gold nanoparticle structure [10] can employ two- and three-dimensional confinement. Generally, plasmonic lasers are characterized by their high metallic loss and low cavity feedback which makes their operation beyond cryogenic temperature impossible.

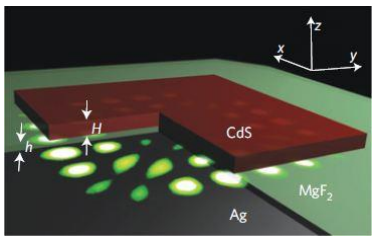

Fig. 1. Physical structure of the Ag-MgF_2-CdS (MIS) approach of room temperature plasmonic laser [11].

Despite being capable of electron injection and compatible with electronic circuit fabrication process, the very low operating temperature requirement of semiconductor plasmonic laser is a major obstacle towards their practical implementation. Low metallic loss, high gain and cavity feedback are needed to make room-temperature operation of plasmonic laser possible. Few attempts have been made towards this direction and one of the experimental works that has already been reported is numerically investigated and evaluated in this work. The laser structure is proposed and tested by Ma et al [11], shown in Fig. 1. This structure consists of 45 nm thick, 1 μm length single crystal CdS square atop a silver surface of 300 nm thickness separated by a 5 nm thick MgF_2 gap layer ensuring $\lambda/20$ optical confinement. In this structure, the feedback mechanism works for only TM mode since the photonic TE mode does not have enough momentum for total internal reflection. As reported, the lasing modes were observed around 500 nm [11].

II. SIMULATION SETUP & METHODOLOGY

In this work, the simulation of the two above-mentioned room temperature plasmonic laser structure is done using Finite-Difference Time-Domain (FDTD) method for solving full-field vector Maxwell's equations. The 'Johnson and Christy' model and sampled data model were used to model Ag and MgF_2 layer, respectively, to correctly reflect dispersion relations of these materials. The simulation setup is shown in Fig. 2a. The CdS gain medium was modelled by a 'four-level two-electron model' [12], as shown in Fig. 2b. The parameters of the model are set as: pump wavelength 405 nm, emission wavelength 500nm, $\mu_{21}= \tau_{30} = 0.1$ ns ($\tau_{21}=$ spontaneous

emission lifetime) [13], $\tau_{32}=\tau_{10}=1$ ps and population density of CdS at room temperature is used. CdS [14] with sampled data was used as the base material four-level two-electron gain medium to accurately model the dispersion relation. The boundary conditions of the computation region were defined as metal and stretched PML. The wavelength and pulse width of the light source were set as 405 nm and 100 fs, respectively. At first, output intensity spectrum due to a unit impulse source was calculated and then multiplied by the Fourier transform of the source signal to obtain the output intensity spectrum due to the total pulse train.

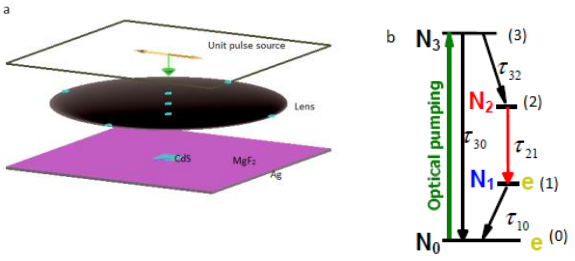

Fig. 2. a. Simulation setup of Ag-MgF_2-CdS (MIS) Structure. b. Four level two electron model of gain medium[12].

III. Simulation Result

Some aspects of the plasmonic laser phenomenon, i.e. modal confinement, are evaluated by calculating effective refractive index of a mode. While the emission spectrum due to a repeated pulse pumping is determined by first calculating the Fourier transform of the unit impulse response then multiplying it with the spectrum of the pumping source. Coupling of the TM mode of the semiconductor slab to the SPPs of the metal surface is determined by calculating effective index and electric-field-intensity distribution along the z axis (Fig. 1). The lasing action is observed by the determining the emission spectrum under different pumping rate.

According to the principle of Plasmonics, the close proximity of the high-permittivity CdS square and silver surface allow the modes of the CdS to couple and share energy with SPPs of the metal dielectric interface, which can be seen in the Fig. 3 where the electric-field-intensity is shown throughout the structure along the z axis. This shows the strong confinement of light in the gap region [15].

The coupling of the optical mode of CdS with surface Plasmon increases the wave-vector and also the momentum, according to the equation, $k_{sp} = k_0\sqrt{\frac{\varepsilon_1\varepsilon_2}{\varepsilon_1+\varepsilon_2}}$ [16]. Where, $\varepsilon_1(\omega)$ is the permittivity of the silver system, ε_2 is the real part of the permittivity of CdS, k_0 and k_{sp} are the wave-vector of the coupled mode of CdS in before and after coupling, respectively. In this case the transverse magnetic field waves (dominant magnetic field of which waves are parallel to the metal surface) couples strongly with the surface plasmons and their momentum increases dramatically. Increase of momentum in turn means increased effective refractive index of the coupled mode. Fig. 4a shows the increase and decrease of effective index of TM and TE modes, respectively, after introducing the silver dielectric layer. This plot is made by calculating effective index of the corresponding modes with the increase of the thickness of the CdS layer. With the increase of the effective index of the TM mode it has sufficient momentum to undergo total internal reflection and obtain necessary feedback for lasing [17,18]. But the TE mode lacks sufficient momentum for total internal reflection and it is also delocalized from surface Plasmon and heavily scattered. The total internal reflection phenomenon is shown in Fig. 4b. Because finite cavity size leads to imperfect internal reflection [19], the laser response is obtained from the volume scattering of radiation waves.

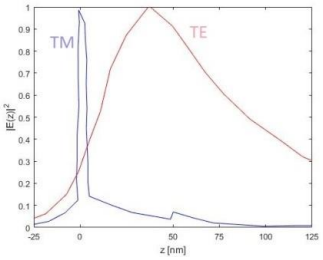

Fig. 3. Intensity distribution of the two modes along the z direction.

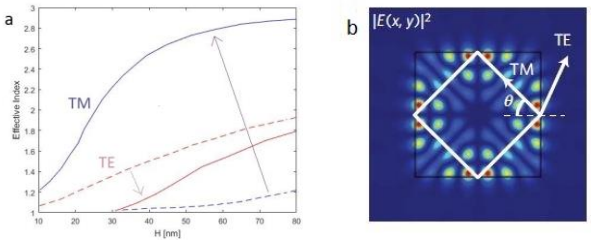

Fig. 4. a. Effective indices for TM and TE modes of CdS square with (solid) and without (dashed line) metal substrate. b. *E* field distribution of a TM mode [11].

Like any other optical resonator, this plasmonic cavity supports a number of modes. The peak of emission spectrum of CdS nanobelt structure is around 500 nm with around 30 nm bandwidth. Those cavity modes whose wavelengths fall under the Photoluminescence curve get amplified. The amplified cavity modes are found by plotting the spontaneous emission spectrum by simulating the system with source of sub-threshold intensity. This emission spectrum is shown Fig. 5a. The Q factor of two pronounced cavity modes 495 nm and 509 nm are 97 and 38. The latter Q factor is an overestimate since this resonance consists of several other modes which are too close to be resolved [11]. Fig. 5b shows the transition between three set of emission spectrum: spontaneous emission spectrum, amplified emission spectrum and full laser emission at pumping rates of 1900 MW cm^{-2} (black), 2200 MW cm^{-2} (red) and 3000 MW cm^{-2} (blue), respectively. At full laser oscillation, a number of higher coherence mode appear due to availability of sufficient energy.

Purcell effect is defined as the enhancement of the spontaneous emission rate of a fluorescent molecule or atom by its environment [21] and it was calculated by the equation (1),

$$F = \frac{\gamma}{\gamma_0} \approx F_\infty[1 + \beta L csch(\alpha L/\sqrt{2})] \quad (1)$$

where, $\gamma = \gamma_{sp} + \bar{Q}B$, γ_{sp} is the enhanced spontaneous emission rate compared to γ_0 the usual emission rate of the CdS band edge transition. Other constants of the equation (1) are taken as, α=6323 cm^{-1}, β=4.93 (μm)$^{-1}$ and F_∞=2.08 [11]. In Fig. 6, the Purcell factor was plotted against the cavity square circumference, L. Simulation result matches the experimented value up to a high degree of accuracy. As the cavity side length decreases cavity feedback increase as the cavity feedback has no effect beyond the surface plasmon propagation length, δ. In this structure high cavity quality factor and strong mode confinement leads to the high Purcell factor as large as 18. This high Purcell factor shows hope in fine investigation of light matter interaction [11].

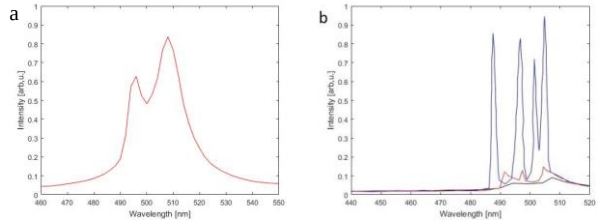

Fig. 5. a. Spontaneous emission spectrum of CdS structure at a peak pump intensity of 1900 MW cm^{-2}. b. Room-temperature laser spectra showing transition from spontaneous emission through amplified spontaneous emission to full laser emission.

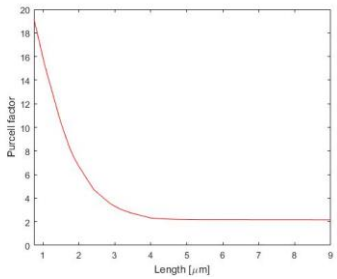

Fig. 6. Plot of the theoretically calculated Purcell factor.

IV. Conclussion

This paper reports the numerical investigation of the performance of an implementation of a room-temperature plasmonic laser. The experimented results are verified in light of classical electromagnetism and semi-classical model of the gain medium. The simulated results were up to the mark of experimental data. This work will hopefully contribute to grow a deeper understanding in this prominent and sophisticated research area.

Acknowledgment

The work is completely performed in the Department of Electrical and Electronic Engineering (EEE), Bangladesh University of Engineering and Technology (BUET), Dhaka, Bangladesh.

References

[1] M. T. Hill et al, "Lasing in metal-insulator-metal sub-wavelength plasmonic waveguides," Opt. express 17, 11107-11112, 2012.

[2] R. F. Outlon, V. j. sarger, T. Zengtagraph, R. M. Ma, C. Gladden, L. Dai, G. Bartal, X. Zhang, "Plasmon lasers at deep subwavelength scale," Nature, vol. 461, pp. 629-632, 2009.

[3] A. V. Akimov et al, "Generation of single optical plasmons in metallic nanowires coupled to quantam dots," Nature Vol. 450, PP. 402-406, 2007.

[4] R. Kolesovet al, "Wave-particle duality of single optical plasmon polaritons," Nature Phys, vol. 5, pp.470-474, 2009.

[5] S. A. Maier, Plasmonics: Fundamentals and applications, Springer, 2007.

[6] A. V. Akimov et al, "Generation of single optical plasmons in metallic nanowires coupled to quantam dots," Nature, vol. 5, pp. 470-474, 2009.

[7] M. T. Hill, M. Marell, E. S. P. Leong, B. Smalbrugge, Y. Zhu, M. Sun, P. J. V. Veldhoven, E. J. Geluk, F. Karouta, Y. S. Oei, R. Nötzel, C. Z. Ning, and M. K. Smit, "Lasing in metal-insulator-metal sub-wavelength plasmonic waveguides," OPt. Express, vol. 17, pp. 11107-11112, 2009.

[8] M. J. H. Marell, B. Smalbrugge, E. J. Geluk, P. J. V. Veldhoven, B. Barcones, B. Koopmans, R. Nötzel, M. K. Smit, and M. T. Hill, "Plasmonic distributed feedback laser at telecommunication wavelegths", Opt. express, vol. 19, pp. 15109- 15118, 2011.

[9] S. H. Kwon, J. H. Kang, C. Seassal, S. K. Kim, P. Regrency, Y. H. Lee, C. M. Lieber, H. G. Park, "Subwavelength plasmonic lasing from a semiconductor nanodisk with silver nanopan cavity", Nano Letters, vol. 10, pp. 3679-3683, 2009.

[10] M. A. Naginov, G. Zhu, A. M. Belgrave, R. Bakkar, V. M. Shalaev, E. E. Narimanov, S. Stout, E. Hertz, T. Suteewong, U. Wiesner, "Demonstration of a spaser based nanolaser", Nature, vol. 460, pp. 1110-1113, 2009, Aug. 2009.

[11] R. M. Ma, R. F. Oulton, V. J. Sorger, G. Bartal and X. Zhang, "Room-temperature sub-diffraction-limited plasmon laser by total internal reflection," NATURE MATERIALS, vol. 10, Feb. 2011

[12] S. H. Chang, A. Taflove, "Finite-difference time-domain model of lasing action in four level two-electron atomic system.", Opt. Express, vol. 12, pp. 3827-3833, 2006.

[13] R. M. Ma, R. F. Oulton, V. J. Sorger, G. Bartal and X. Zhang," Supplementary Information" on "Room-temperature sub-diffraction-limited plasmon laser by total internal reflection," NATURE MATERIALS, vol. 10, Feb. 2011.

[14] Refractive index of CdS (Cadmium sulfide)- Treharne. [Online], Available: https://refractiveindex.info/?shelf=main&book=CdS&page=Treharne

[15] R. F, Outlon, V. J. Sorger, D. A. Genov, D. F. P. Pile, and X. A. Zhang, "A hybrid plasmonic waveguide for subwavelength confinement and long-range propagation," Nature Photon, vol. 2, pp. 496-500, 2008.

[16] W. L. Barnes, A. Dereux, and T. W. Ebberson, "Surface plasmon subwavelength optics" Nature,VOL 424,Aug. 2003.

[17] A. W. Poon, F. Courvoisier and R. K. Chang, "Multimode resonance in square-shaped optical microcavities," Opt. Letter, vol. 26, pp. 632-634, 2001.

[18] Y. Z. Huang, Q. Chen, W. H. Guo, L. J. Yu, "Experimental observation od resonant modes in GaInP microsquare resonators," IEEE Photonics Technol. Letter, vol. 17, pp. 2589-2591, 2005.

[19] J. Wiersig, "Formation of long lived, scarlike modes near avoided resonance crossings in optical microcavities," Phys. Rev. Letter, vol. 97, pp. 253901, 2006.

[20] B. Liu, R. Chen, X. L. Xu, D. H. Li, Y. Y. Zhao, Z. X. Shen, Q. H. Xiong, H. D. Sun,"Exciton related photoluminescence and lasing in CdS nanobelts," Journal of physical chemistry, vol. 115, pp. 12826-12830, 2011.

[21] Purcell Effect - Wikipedia, [Online], Available: https://en.wikipedia.org/wiki/Purcell_effect